CHAOS 21, 033109 (2011)

Stability, bifurcations, and dynamics of global variables of a system of bursting neurons

Igor Franović,[1] Kristina Todorović,[2] Nebojša Vasović,[3] and Nikola Burić[4,a)]
[1]Faculty of Physics, University of Belgrade, P.O. Box 44, 11001 Belgrade, Serbia
[2]Department of Physics and Mathematics, Faculty of Pharmacy, University of Belgrade, Vojvode Stepe 450, 11221 Belgrade, Serbia
[3]Department of Applied Mathematics, Faculty of Mining and Geology, P.O. Box 162, 11000 Belgrade, Serbia
[4]Scientific Computing Lab., Institute of Physics, University of Beograd, P.O. Box 68, 11080 Beograd-Zemun, Serbia

(Received 1 February 2011; accepted 11 July 2011; published online 5 August 2011)

An approximate mean field model of an ensemble of delayed coupled stochastic Hindmarsh-Rose bursting neurons is constructed and analyzed. Bifurcation analysis of the approximate system is performed using numerical continuation. It is demonstrated that the stability domains in the parameter space of the large exact systems are correctly estimated using the much simpler approximate model. © *2011 American Institute of Physics*. [doi:10.1063/1.3619293]

Bursting is a neuronal activity such that a neuron fires two or more spikes followed by a period of quiescence, which is again followed by similar periods of spiking and quiescence. This type of neuronal dynamics is quite common and has been observed in the activity of single neuron as well as in the activity of small parts of the brain cortex. Inter-neuronal interaction time delay and noise are known to have profound effects on the dynamics of few coupled neurons. Such systems are mathematically described by a collection of nonlinear stochastic delay-differential equations, where analytical solutions are impossible and numerical treatment is quite ineffective. In order to analyze the combined effects of the time-delay and the noise on the dynamics of large ensembles of neurons, one needs effective and sufficiently good approximate models. We have analyzed a large set of Hidmarsh-Rose bursting neurons modulated by noise and coupled via the time-delayed electrical synapses. The global coarse-grained dynamics of the system is described by the collective averaged variables. We have used typical assumptions of the mean field approximation to derive the set of nine deterministic delay-differential equations for the first and the second moments of the collective variables. Bifurcations due to variations of different parameters, characterizing the time-lag, interaction strength, and the noise intensity, are observed in the dynamics of global variables of the exact system with large number of units, and the bifurcation values are compared with those predicted by the approximate model with only nine deterministic equations. Domains in the parameter space corresponding to stable quiescent behavior or to the bursting of the collective variables of the large exact system are correctly predicted by the approximate model.

I. INTRODUCTION

Bursting is an important dynamical state of a real neuron and of collections of such neurons. It is believed that a burst of spikes is more reliable than a single spike in producing responses in postsynaptic neurons.[1] Small parts of the brain cortex may contain thousands of morphologically and functionally similar interconnected bursting neurons and each of them is mathematically modeled by few nonlinear differential equations.[1–3] Dynamics of such neuronal network is crucially influenced by the interaction, i.e., synaptic delays[4,5,7–10] (and[6] the references therein), and by small perturbations of various origins which are commonly treated as noise.[11,16]

It is clear that relatively detailed mathematical model of a small part of realistic cortex should involve an extremely large system of nonlinear stochastic delay-differential equations (SDDEs). Analysis of such complex models is impossible, even with the help of modern supercomputers, without more or less severe approximations. Our main goal in this paper is to develop an approximation of large ensemble of coupled bursting neurons and to demonstrate that bifurcation analysis of the approximate model is possible and provides useful information about the exact large system.

Delay-differential equations (DDEs) with noise do not satisfy the Markov assumption[18,19] which complicates their analysis. Stability of such SDDEs has been studied using extensions of the Lyapunov method long time ago,[18] but with little influence in applications apart from models of mechanical devices. More recently, stability of synchronization in systems with noise involving DDE was studied analytically in the context of coupled realistic and formal neural networks. Liao and Mao[20] (see also Ref. 19) have initiated the study of stability in stochastic neural networks and this was extended to stochastic neural networks with discrete time-delays in Refs. 21 and 22. Some analytical techniques relevant for delayed systems with noise have also been used in the study of coupled bistable systems with delays[23] and in noisy oscillators with delayed feedback.[24,29] Small world and scale free networks of various neuronal models with noise and synaptic delays have been studied numerically, for example, in Refs. 30–35.

Our approximation is based on ideas and assumptions of the mean field approach. The mean field approximation

a)Electronic mail: buric@ipb.ac.rs.

 © 2011 American Institute of Physics

(abbreviated MFA) has been applied on systems of excitable neurons with noise but with no time-delay, for example, in Refs. 13 and 36–38 Otherwise a type of MFA was devised in Refs. 39 and 40 and applied on large clusters of noisy neurons with time-delayed interaction in Ref. 41. Global dynamics of a system of delayed coupled noisy 1D elements was recently studied using the mean field approach in Ref. 42. Recently, an analytically tractable MFA for delayed-coupled noisy excitable FitzHugh-Nagumo neurons was developed[43] and used.[44] The mean field approximate model developed here, in Sec. II, is still too complicated for an analytic treatment, but the numerical bifurcation analysis, presented in Sec. III, is possible and the results of such analysis are the main topic of our paper.

II. THE EXACT LARGE SYSTEM AND ITS APPROXIMATE MODEL

Different types of bursting activity have been observed in real single neuron and collections of neurons.[1] Typical example of bursting dynamics is provided by the three dimensional model proposed by Hindmarsh and Rose (HR),[45]

$$\begin{aligned} dx/dt &= F_x = y + 3x^2 - x^3 - z + I,\\ dy/dt &= F_y = 1 - 5x^2 - y,\\ dz/dt &= F_z = -rz + rS(x - C_x), \end{aligned} \tag{1}$$

where x is the membrane potential, y represents the fast current, like N_a^+ or K^+, and z represents the slow current, for example, Ca^{2+}. r, S, and b are parameters which are in this paper set to constant typical values, $r = 0.0021$, $S = 4$, and $C_x = -1.6$. The HR equations (1) describe the dynamics of a single neuron subjected to an external stimulus I. Depending on the values of the parameters r, S, C_x, and the current I, the model can have qualitatively different attractors corresponding to quiescent state, periodic firing, and bursting with regular or chaotic sequences of bursts.[46,47] The bursting dynamics is driven by the oscillations of the slow z variable and occurs once they acquire sufficiently large amplitude, which is preferably induced by supplying an appropriate external stimulus I. The bursts of spikes endure during the period when z is increasing and the stable quiescent state is observed, while $dz/dt < 0$.

In this paper, we shall analyze the bursting dynamics of collective variables in an ensemble of HR neurons. The model explicitly includes the interaction delays and stochastic perturbation represented by additive white noise and is given by the following system of $3N$ SDDE:

$$\begin{aligned} dx_i &= [F_x(x_i, y_i, z_i) - \frac{1}{N}\sum_j^N c(x_i - x_j(t-\tau))]dt + \sqrt{2D}dW,\\ dy_i &= F_y(x_i, y_i, z_i)dt,\\ dz_i &= F_z(x_i, y_i, z_i)dt, \quad i = 1, 2 \ldots N, \end{aligned} \tag{2}$$

where F_x, F_y, F_z are given by Eq. (1). There are two major types of inter-neuronal couplings: the chemical and the electrical synapses. Time-delay τ is important especially in the first type of synapses, but plays also an important role in the electrical junctions and in the transmission of an impulse through the dendrite. In Eq. (2), we use the electrical coupling with the time-lag τ and the strength c that is equal for all pairs of neurons. The assumption that all internal neuronal parameters and all coupling constants are equal is plausible if the neurons are found in a small patch of the brain cortex. The collective dynamics of such an ensemble of closely placed neurons would then be monitored by a single electrode in an electroencephalographic (EEG) recording.

The terms $\sqrt{2D}dW_i$ represent stochastic increments of independent Wiener processes, i.e., dW_i satisfy

$$E(dW_i) = 0, \quad E(dW_i dW_j) = \delta_{i,j}dt, \tag{3}$$

where $E(\cdot)$ denotes the expectation over many realizations of the stochastic process. The intensity of the noise D and the stochastic properties of the noise are assumed to be the same for all neurons, but, of course, single realizations of the Wiener processes in the equations for x_i need not be the same functions of t for all i. Noise could be added also in the other equation of the fast subsystem. It is known that, in the case of excitable systems, the noise in the dx_i equation or in the dy_i equation produce different types of stochastic coherence effects.[50] The mean field approach, presented in this paper, could be applied equally with almost no modification, if the noise term was in the dy_i equation or in both dx_i and dy_i equations. Nevertheless, we arbitrarily decided to treat the case with the noise in the dx_i equation.

Before we start with the analysis of the system (2) with a large number of units, it is instructive to recapitulate the synchronization properties of the system with only two neurons.[5,26,48] Transition from the quiescent or simple oscillatory state to bursting dynamics of two HR neurons can be induced either by increasing the external parameter I, the coupling strength $|c|$, the noise D, or the time-lag τ. The bursting of the two neurons can be exactly synchronous, i.e., $x_1(t) = x_2(t)$, approximately synchronous $x_1(t) \approx x_2(t)$, or completely asynchronous. Sufficiently strong coupling with zero or small delay usually induces synchronization, which remains an approximate one as long as the noise is not too large. Non-zero time-lag in a specific interval can induce synchronization of weakly coupled deterministic bursters, but the synchronization completely disappears with the addition of a very small noise if the coupling remains weak. As for the synchronization in systems with a large number of noiseless and instantaneously coupled bursters, it is known that the synchronization can be achieved with weak coupling if each of the neurons is connected with (equal) sufficiently large number of other neurons.[49] As we shall see, these facts are reflected in the properties of global bursting dynamics of the system with large N.

A. The mean field approximation

We are interested in the dynamics of the global averaged variables of the large system (2). These are defined as the space averages,

$$m_x(t) = 1/N\sum_i^N x_i(t) \equiv \langle x_i(t)\rangle,$$
$$m_x(t-\tau) = 1/N\sum_i^N x_i(t-\tau) \equiv \langle x_i(t-\tau)\rangle,$$
$$m_y = 1/N\sum_i^N y_i \equiv \langle y_i\rangle,$$
$$m_z = 1/N\sum_i^N z_i \equiv \langle z_i\rangle. \quad (4)$$

In order to obtain a closed system of equations for the spatial averages and correlations, we need several assumptions typical of the mean field approach. The assumptions are formulated using the centered first moments,

$$n_{x_i}(t) = m_x(t) - x_i(t), \quad n_{y_i}(t) = m_y(t) - y_i(t), \quad n_{z_i}(t) = m_z(t) - z_i(t), \quad (5)$$

and assume that they are statistically independent in different units. Next, mean square deviations,

$$s_x(t) = \langle n^2_{x_i}(t)\rangle, \quad s_y(t) = \langle n^2_{y_i}(t)\rangle, \quad s_z(t) = \langle n^2_{z_i}(t)\rangle, \quad (6)$$

and cross-cumulants,

$$u_{xy} = \langle n_{x_i}n_{y_i}\rangle, \quad u_{xz} = \langle n_{x_i}n_{z_i}\rangle, \quad u_{yz} = \langle n_{y_i}n_{z_i}\rangle, \quad (7)$$

are introduced.

Next, we shall assume that for sufficiently large N, the global space averages (4) of local quantities, say $m_x(t)$, are equal to the expectations with respect to distribution of the corresponding variable $E(x_i(t))$. Because of the assumed Gauss distribution of each variable, the first and the second order cumulants of the deviations (5) are equal to the first and second order centered moments of the variables x_i, etc. Due to the same Gaussian assumption, cumulants of order higher than second are equal to zero.

The well known formulas of the cumulant expansion up to the fourth order[17] are used to obtain, after some algebra, the expressions for higher order auto-correlations. In particular,

$$\begin{aligned}
\langle x_i^2(t)\rangle &= s_x(t) + m_x^2(t),\\
\langle x_i(t)^3\rangle &= m_x^3(t) + 3m_x(t)s_x(t),\\
\langle x_i^4(t)\rangle &= m_x^4(t) + 6m_x^2(t)s_x(t) + 3s_x^2(t),\\
\langle x_i(t)y_i(t)\rangle &= u_{xy}(t) + m_x(t)m_y(t),\\
\langle x_i^2 y_i\rangle &= m_y s_x + m_y m_x^2 + 2m_x u_{xy},\\
\langle x^3 y\rangle &= 3s_x u_{xy} + 3s_x m_x m_y + 3m_x^2 u_{xy} + m_y m_x^3,\\
\langle xyz\rangle &= U_{xy}m_z + u_{yz}m_x + u_{xz}m_y + m_x m_y m_z,\\
\langle x^2yz\rangle &= s_x m_y m_z + m_x^2 u_{yz} + m_x^2 m_y m_z + 2u_{xz}u_{xy}\\
&\quad + 2u_{xz}m_x m_y + 2m_x m_z u_{xy} + s_x u_{yz}.
\end{aligned} \quad (8)$$

Using the first three equations of Eq. (8) and the assumption that the spatial average for large N is equal to the stochastic average, the spatial average of Eq. (2) becomes

$$\begin{aligned}
\dot m_x(t) &= -(m_x^3(t) + 3m_x(t)s_x(t)) + 3(s_x(t) + m_x^2(t))\\
&\quad + m_y(t) - m_z(t) + I + c(m_x(t-\tau) - m_x(t)),\\
\dot m_y(t) &= 1 - 5(s_x(t) + m_x^2(t)) - m_y(t),\\
\dot m_z(t) &= r(S(m_x(t) - C_x) - m_z(t)).
\end{aligned} \quad (9)$$

In order to close the system (9), we need the evolution equations for $s_x(t)$. This involves other second moments, and the corresponding evolution equations are obtained using the Ito chain rule[17] and Eq. (8). The second moments satisfy

$$\begin{aligned}
\dot s_x(t)/2 &= s_x(t)[6m_x(t) - 3m_x^2(t) - 3s_x(t) - c]\\
&\quad + u_{xy}(t) - u_{xz}(t) + D,\\
\dot s_y(t)/2 &= -10m_x(t)u_{xy}(t) - s_y(t),\\
\dot s_z(t)/2 &= Sru_{xz}(t) - rs_z(t),\\
\dot u_{xy}(t) &= u_{xy}(t)[6m_x(t) - 3s_x(t) - 3m_x^2(t) - 1 - c]\\
&\quad - 10m_x(t)s_x(t) + s_y(t) - u_{yz}(t),\\
\dot u_{xz}(t) &= u_{xz}(t)[6m_x(t) - 3s_x(t) - 3am_x^2(t) - r - c]\\
&\quad - s_z(t) + rSs_x(t),\\
\dot u_{yz}(t) &= rSu_{xy}(t) - u_{yz}(t)(1+r) - 10m_x(t)u_{xz}(t).
\end{aligned} \quad (10)$$

Following the next step in the analogous, analysis of the large system of excitable two dimensional FitzHugh-Nagumo neurons[43] (see also the analsis of the FitzHugh-Nagumo neurons without the time-delay in Refs. 13 and 38) would consists in substitution of the stationary values for the second moments of Eq. (10) into the Eq. (9) of the first moments. However, due to relatively complicated form of the right-hand sides of Eq. (10), the resulting three equations for the first moments would still be quite difficult to analyze. Instead, we shall use the numerical continuation method to perform bifurcation analysis of the system of 9 DDEs (9) and (10). Predictions of this analysis will then be compared with numerical solutions of the exact large system.

III. NUMERICAL STABILITY AND BIFURCATION ANALYSIS OF THE APPROXIMATE SYSTEM

Our goal in Sec. IV will be to demonstrate that the qualitative agreement of the approximate and the exact system extends over a large range of parameters I, c, τ, and for relatively small noise D, so that qualitatively different types of the exact dynamics are correctly reproduced by the approximate system. Let us stress that our claim will not be that the time series produced by the exact and the approximate equations are quantitatively similar, but we shall claim that the approximate equations correctly predict the qualitative type of dynamics for parameters in the specified domains.

Given that the complexity of the approximate model seriously compromises, if not precludes an analytical treatment, one is compelled to consider some means of numerical bifurcation analysis. Before turning to details, let us point out that the destabilization of equilibrium generically occurs via the subcritical Hopf bifurcation. However, this does not rule out the existence of the more subtle secondary bifurcation phenomena in certain parameter domains, viz., the Bogdanov–Takens point is indicated for very small weights under the moderate stimuli and delays. Focussing on the subcritical Hopf bifurcation, the destabilization scenario consists in that an unstable limit cycle collapses on a stable fixed point making it unstable, whereas passed the bifurcation parameter value the trajectory moves over to a stable limit cycle, located further away in the phase space. Within this setup, the onset of bursting coincides with a pair of conjugate characteristic roots crossing the imaginary axes. The numerical analysis is carried out by implementing the DDE-biftool, which is a package of flexible Matlab routines appropriate for handling the systems of differential equations with constant delays.[52,53] The calculation of the stability-determining characteristic roots itself involves two stages: the first, posing the approximation by the linear multi-step method, and the correction one, which rests on the Newton iteration method. Most notably, the software allows for numerical continuation over the Hopf bifurcation point, making it possible to switch to an emanating branch of periodic solutions.

The derived bifurcation curves, displayed in Fig. 1, are intended to demonstrate how the interplay of I, c, D, and τ affects the destabilization of equilibrium for the approximate model, whereby the fixed point is stable (unstable) below (above) each of the curves. For instance, from Fig. 1(a), one reads that under the action of small stimuli, only excessive delays give rise to destabilization if $|c|$ is decreased. Nonetheless, at moderate τ, the bifurcation values of I show a sharp rise for smaller c, whereas they virtually reach saturation in the absence of noise (not shown) or exhibit a very slow growth once a small amount of noise is introduced, see Fig. 1(b). Finally, from Fig. 1(c), we learn that for intermediate I and τ, the stronger the weights become, the larger D is required to destabilize the equilibrium. To reiterate, the formulation of the approximate model is justified if it yields the correct stability behavior of the equilibrium as compared to the exact system, a point witnessed later on by plotting the corresponding factual time series for the parameter values below and above the obtained bifurcation curves.

IV. NUMERICAL ILLUSTRATIONS

For most part of our computations, we have applied the Euler method of numerical integration, though at some instances, the Runge-Kutta fourth and fifth order routines for the deterministic part of Eq. (2) have also been implemented. The results are compared with those obtained by the ready-made programs for solving SDDE provided in the XPP package.[51] Many sample paths of Eq. (2) for the same parameter values have been computed, but in figures, we represent the global variable $X(t)$ along the parts of only one typical sample path and compare these with numerical solutions of the approximate system of DDEs (9) and (10).

A system of delay differential equations with the time-lag τ is an infinite dynamical system, and the corresponding initial conditions are given by continuous functions on the interval $[-\tau,0]$. In what follows, we shall always use as the initial functions the solutions of Eqs. (2) or (9) and (10) with

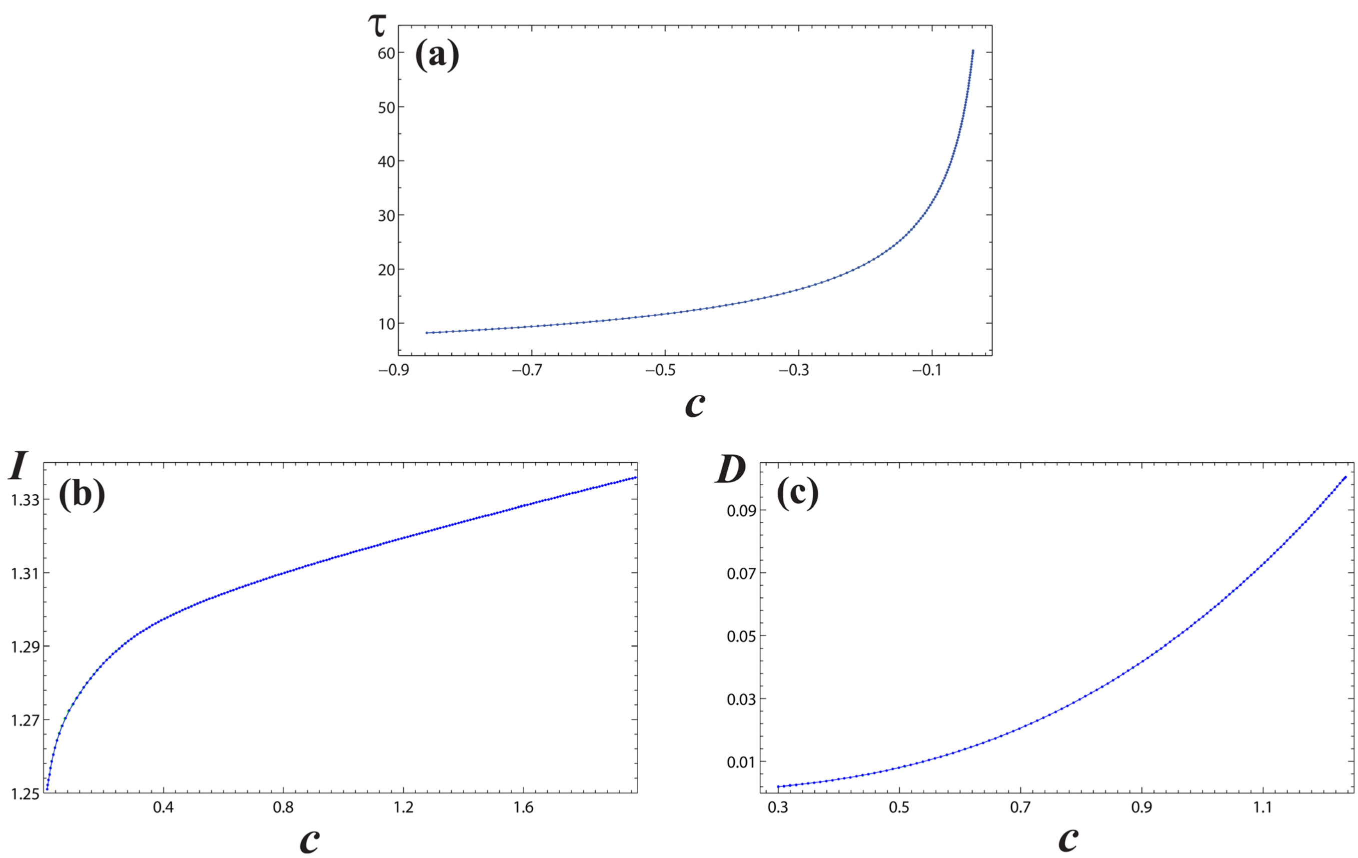

FIG. 1. (Color online) Bifurcation diagrams for the approximate model reflecting the destabilization of equilibrium via the Hopf bifurcation. Subfigures (a), (b), and (c) focus on the $\tau(c)$, $I(c)$, and $D(c)$ dependencies, respectively. The fixed point is stable (unstable) below (above) each of the curves. The remaining parameter values are $I = 1.25$, $D = 0$ in (a), $\tau = 8$ and $D = 0.001$ in (b), as well as $I = 1.29$, $\tau = 10$ in (c).

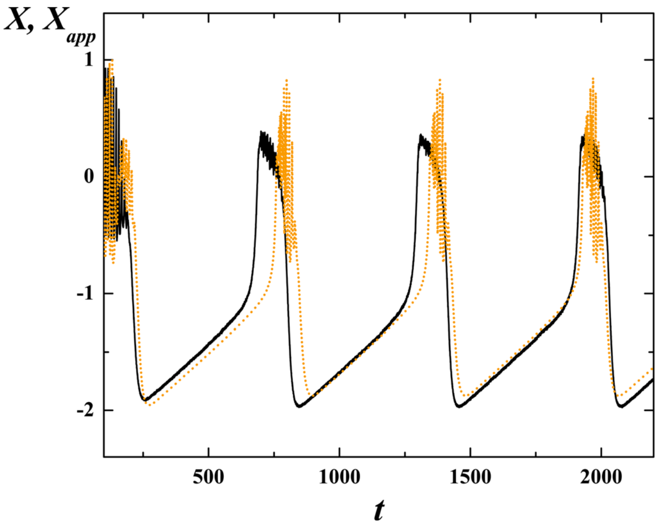

FIG. 2. (Color online) Examining whether there are parameter regions that favor precise matching between $X(t)$ and $X_{app}(t)$, provided the initial conditions are analogous. Throughout the paper, we adhere to a representation scheme where the exact series are shown by the black solid lines, while the approximate data are displayed by the dotted lines, coded orange (light gray). Contrary to the common logic, there are instances of close quantitative agreement of the data sets even under large D. Here, the parameter values are $N = 200$, $I = 1.3$, $c = 1$, $\tau = 10$, and $D = 0.04$.

$c = 0$ and with specified values of the variables at $t = 0$. If the values of a given local variable at $t = 0$ are equal for all i, we shall say that the initial data are equal, and if the local values at $t = 0$ are Gauss distributed, we shall say that the initial data are Gauss distributed. In this case, the initial data for Eqs. (9) and (10), i.e., the values of the first and the second moments at $t = 0$, are fixed by the Gaussian distribution of the local variables.

Of course, the dynamics of the global variables along the sample paths of the exact system (2), which is stochastic for $D \neq 0$, can not be exactly reproduced by the orbits of the deterministic approximate models (9) and (10). However, the qualitative dependence on the parameters and their bifurcation values are still well predicted. Furthermore, the difference between the values of the global variables on different sample paths for the same values of the parameters is already at $D = 0.001$ of the same order as the difference between the values given by the approximate model and any of the sample paths.

Apart from the qualitative agreement between the exact system and the approximate model in terms of equilibrium destabilization, an additional gain would be to determine whether there are parameter regions that warrant the close quantitative match between the corresponding time series of global potentials, designated X and X_{app} in the remainder of the paper. By common logic, one expects this to be fulfilled in the absence of noise. However, the comparison of the data obtained for the exact system extended to $N = 200$ neurons and the approximate model (Fig. 2) under the analogous initial conditions shows the two series converging irrespective of the large D. Here, it should be cleared out that the exhibited tendency persists beyond the displayed time interval. Such an outcome makes it explicit how the possible overlap between $X(t)$ and $X_{app}(t)$ is also influenced by the parameters other than noise, notably the stimulation current. What matters about the particular value $I = 1.3$ is that it would be sufficient to induce bursting in the noiseless case if the rest of parameters were to remain as in Fig. 2.

In view of the stated above, we proceed to the analysis of the sets of data provided by the exact system and the approximate model under the analogous initial conditions. The results are compared for the parameter values lying below and above the bifurcation curves from Fig. 1. The validity of the $\tau(c)$ dependence displayed in Fig. 1(a) is exemplified by the time series in Fig. 3, where the delay is gradually

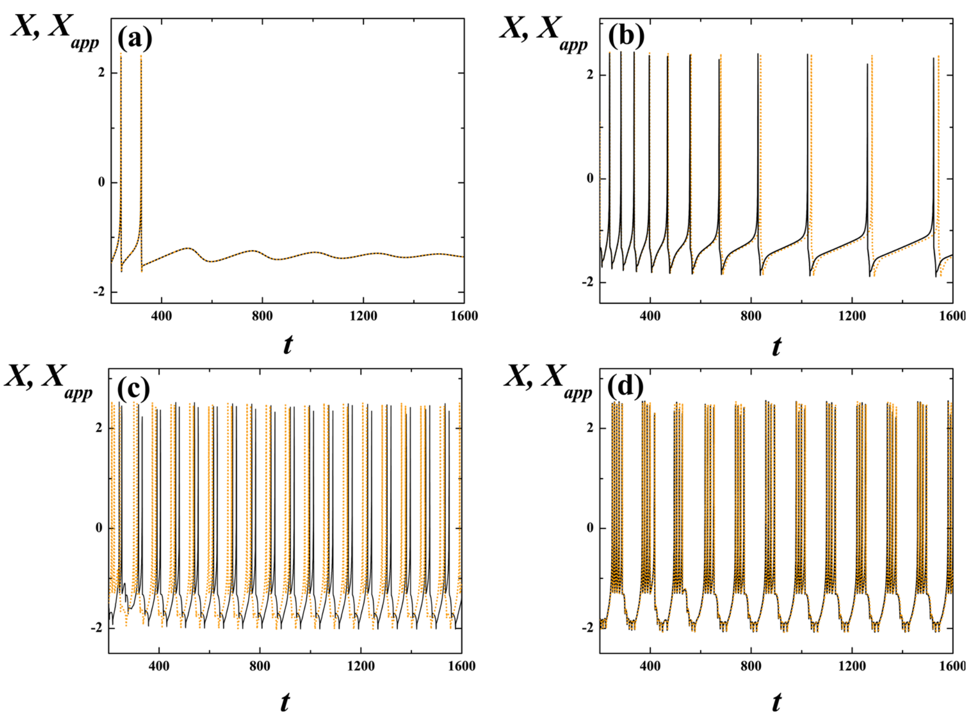

FIG. 3. (Color online) Destabilization of equilibrium under the increase of τ. We argue for the qualitative agreement between the approximate model and the exact system in a sense that their time series should reflect how the fixed point is stable (unstable) for the parameter values lying below (above) the bifurcation curve in Fig. 1(a). For sub-bifurcation delay $\tau = 2$ in (a), the quiescent behavior is asymptotically stable. Once above the bifurcation value, the neurons first engage in periodic bursting, as seen at $\tau = 9$ in (b), whereas further enhancing the delay gives rise to bursting shown for $\tau = 25$ in (c) and $\tau = 50$ in (d). The remaining parameters take values $I = 1.25$, $c = -0.8$, $D = 0$, and $N = 70$.

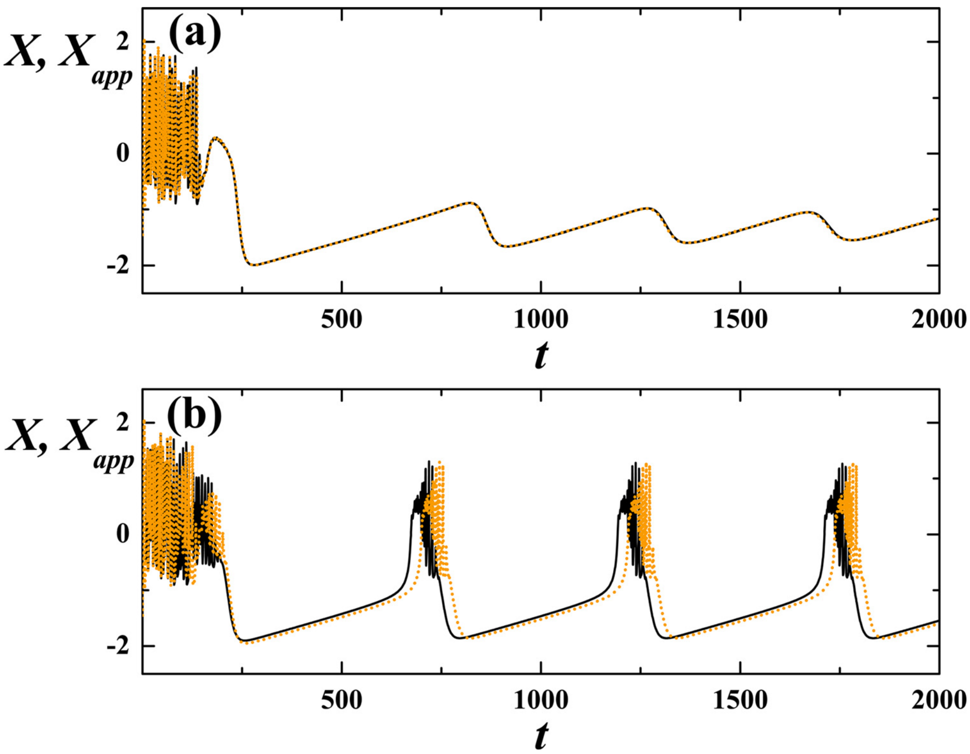

FIG. 4. (Color online) System dynamics undergoes transition from asymptotically stable quiescence to bursting under the increase of I in correspondence to the bifurcation diagram displayed in Fig. 1(b). $X(t)$ and $X_{app}(t)$ under the analogous initial conditions are obtained for $I = 1.29$ in (a) and $I = 1.32$ in (b), with the rest of parameters being $\tau = 8$, $c = 1$, $D = 0.001$, and $N = 70$.

increased keeping the remaining parameters fixed. For τ below the bifurcation threshold, there are only relaxation oscillations of the global potentials X and X_{app}, whereas just above it, one encounters the fixed point destabilized, as the regime of periodic spiking sets in. Further enhancement of τ leads to an onset of bursting. Aside from the fact that the approximate model reproduces all of the major regimes exhibited by the exact system, it strikes that the approximate series seem to best fit the exact one for very large $\tau = 50$.

Figure 4 illustrates the qualitative agreement between the data obtained and the $I(c)$ dependence from Fig. 1(b). Again, we find the damped oscillations below the bifurcation current and the bursting regime taking place above it. In the former case, $X(t)$ and $X_{app}(t)$ provide an excellent match under the analogous initial conditions, whereas they are slightly shifted in the latter. On the qualitative side, the above argument also holds up for the displayed in Fig. 5 that relates to the $D(c)$ bifurcation diagram in Fig. 1(c). However, the greatest departing so far between the approximate model and the exact system deserves some additional attention. The reason behind this lies in the stimulus value $I = 1.29$, which, connoted with the remaining set of parameters, makes the induced bursting exclusively noise-driven. With this in mind, one cannot expect the deterministic approximate system to replicate the exact dynamics of the stochastic one with any significant fidelity. On a final note, the proposed approximate model is put to the test by considering the noiseless and the delay-free case, where the perfect match with the exact series should occur. To this end, we compared the data obtained for the damped oscillations and the bursting regime, recovering a complete agreement in either event (see Fig. 6).

All the examples of the different dynamical phenomena illustrated so far have been obtained for relatively strong coupling $c = 1$ or $c = -0.8$ between the neurons. Figure 7 is intended to illustrate the changes introduced by decreasing the coupling. Strong coupling prompts synchronization between the neurons which is only slightly perturbed by small noise. Thus, the local bursters discharge in an almost synchronous fashion and the global averages also display clear burst with large amplitude. This is illustrated in Figs. 7(a)–7(c) by showing only one burst in the exact dynamics of $X(t)$, the dynamics of its approximation $X_{app}(t)$ and $x_1(t)$ versus $x_8(t)$. $X_{app}(t)$ is qualitatively similar to $X(t)$, and all pairs of local bursters $x_i(t)$, $x_j(t)$ are almost synchronous. On the other hand, weak coupling also implies synchronous dynamics of local bursters with zero noise, but this synchrony is completely destroyed by arbitrarily small noise. Because of this noise induced de-synchronization, the global variables only display dumped bursting as is illustrated in Fig. 7(d). The stationary state is unstable, but the individual bursting is de-synchronized, so that spatial averaging only produces dumped bursting in global variables. The approximate model correctly predicts that the stationary state is unstable, but it undergoes clear bursting dynamics which is quantitatively different from the exact system global variables. Figure 7(f) shows that the weakly coupled local bursters are completely de-synchronized by the small noise.

It is expected that the estimates of the critical parameter values corresponding to different bifurcations that are provided by the approximate models (9) and (10) become more accurate as the number of units of the exact system is increased. For example, consider the transition from the bursting dynamics (with the unstable stationary state) that occurs in the approximate system for the fixed parameter values, $\tau = 8$, $c = 1$, $D = 0.001$, somewhere between $I = 1.275$ (stable, no bursting) and $I = 1.295$ (unstable, bursting). This transition occurs in exact system with

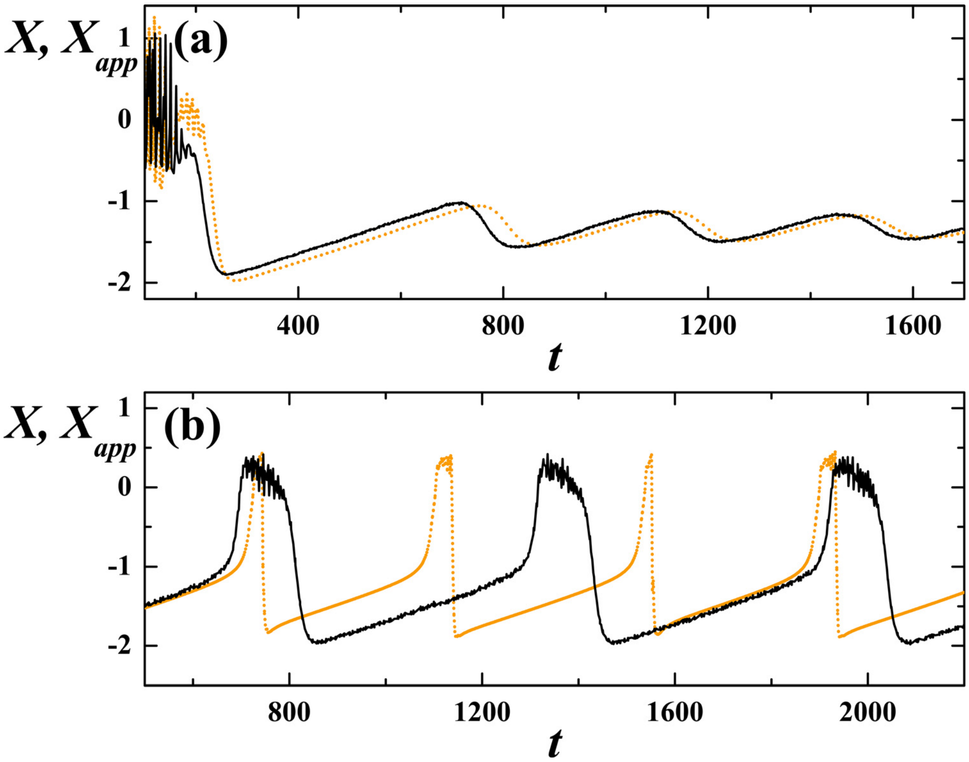

FIG. 5. (Color online) Prompted by the increasing noise, the system dynamics undergoes transition from stable quiescent behavior to bursting, as anticipated by the bifurcation diagram in Fig. 1(c). The noise values are $D = 0.01$ in (a) and $D = 0.057$ in (b), with the remaining parameters set at $I = 1.29$, $\tau = 10$, and $N = 70$. $X(t)$ and $X_{app}(t)$ depart from each other, in particular, for the ascending and the descending sections of bursts being much sharper in the latter, as the observed transition is exclusively driven by noise.

$N = 70$ for the same parameter values and in the indicated interval of I. This is illustrated in Fig. 8. On the other hand, the exact system with $N = 65$ for the same fixed parameters and for $I = 1.275$ has an unstable stationary state and the global dynamics displays bursting. For $N = 65$, the cessation of bursting and stabilization of the stationary state occurs somewhere between $I = 1.22$ (stable, no bursting) and $I = 1.23$ (unstable, bursting). The critical value of I for $N = 50$ is between $I = 1.2$ (stable, no bursting) and $I = 1.22$ (unstable, bursting), which is even further away from the value estimated with the approximate system than in the $N = 65$ case. For $N = 10$ the transition occurs between

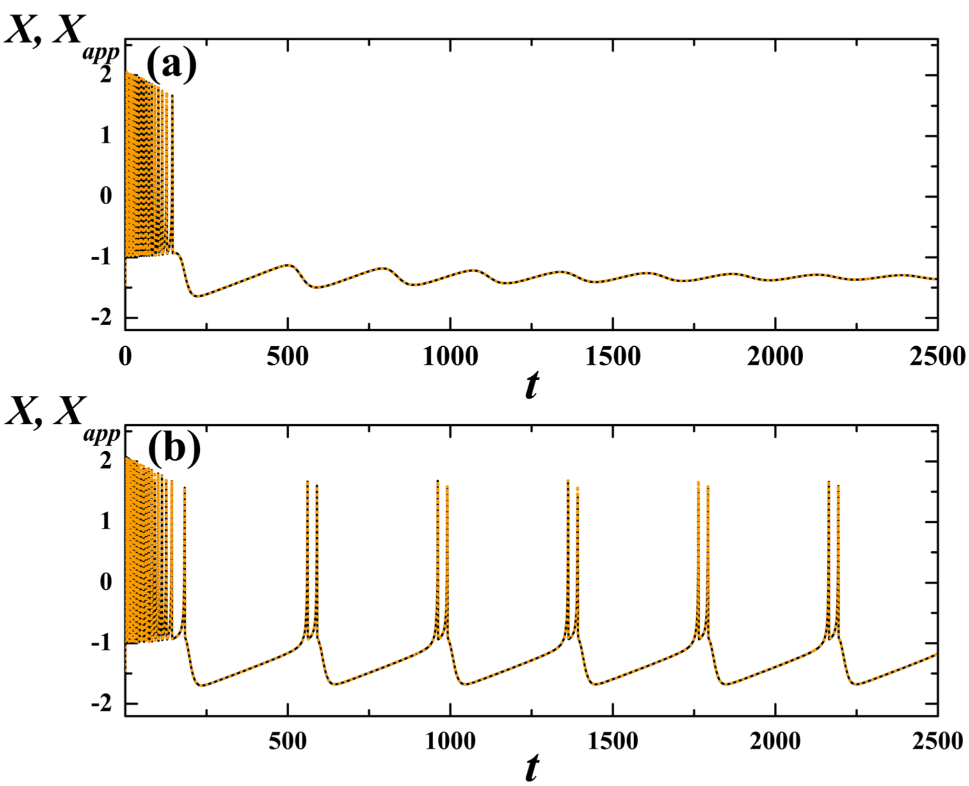

FIG. 6. (Color online) Comparison between $X(t)$ and $X_{app}(t)$ under the analogous initial conditions in the noiseless and the delay-free case. Increasing I, there is an excellent agreement both for the damped oscillations and the bursting regime. The results are presented for $I = 1.265$ in (a) and $I = 1.272$ in (b), with the remaining parameters being $c = 1$ and $N = 70$.

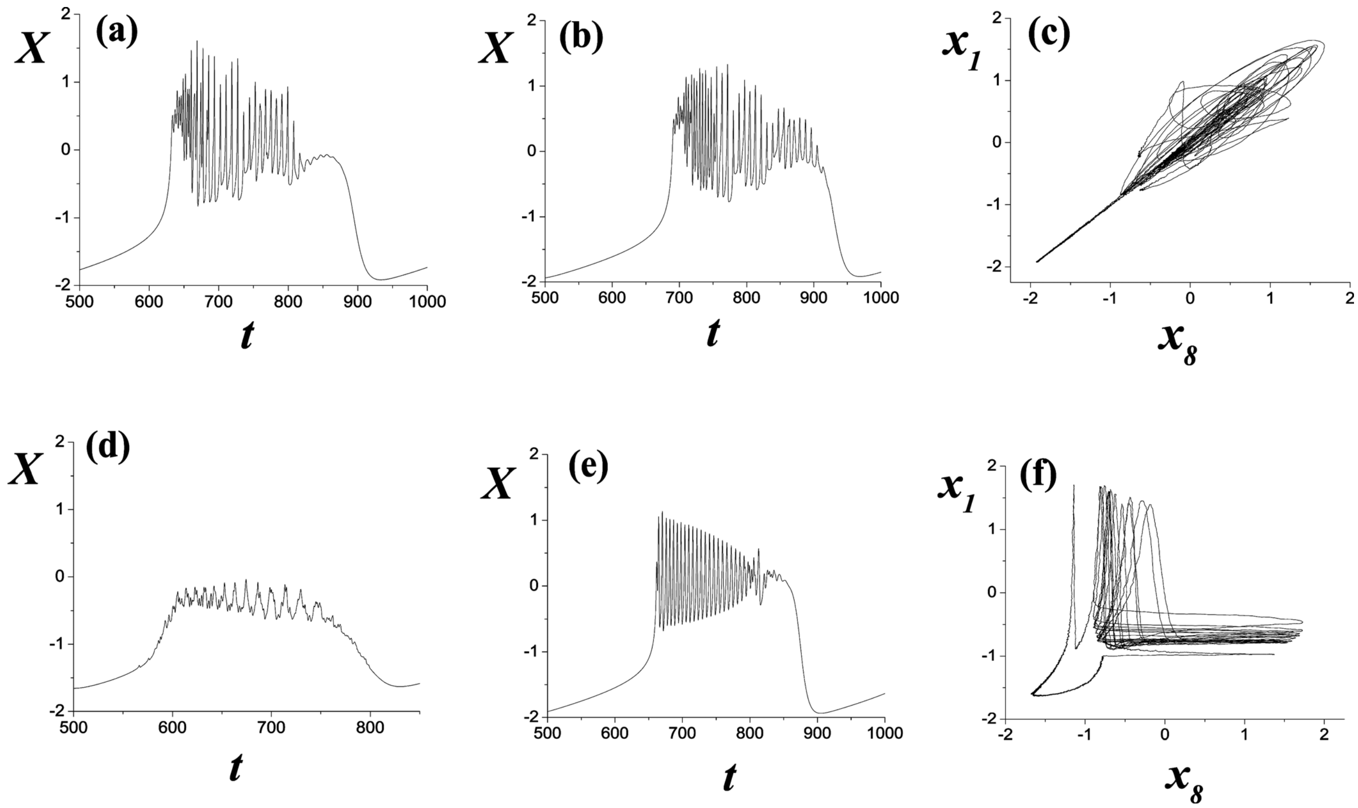

FIG. 7. Illustrates the influence of the coupling strength c on the bursting global dynamics in the case when the parameters $I = 3$, $\tau = 0$, $D = 0.001$ are such that each individual neuron is bursting. In (a) (exact) and (b) (approximate), $c = 1$ and in (d) and (exact) (e) (approximate), $c = 0.1$. In (c) $c = 1$ and (f) $c = 0.1$, $x_1(t)$ vs. $x_8(t)$ are shown.

$I = 1.15$ (stable, no bursting) and $I = 1.17$ (unstable bursting). We see that, as expected, the estimated critical value becomes more accurate as the number of units in the exact system is increased.

V. SUMMARY AND DISCUSSION

We have studied stability and bifurcations that induce the bursting dynamics of the global variables of a large ensemble of coupled bursting neurons. Each of the neurons is represented by Hidmarsh-Rose model which is known to be able to display the bursting dynamics for sufficiently strong external perturbation. Influence of noise is modeled by additive white noise in each neuron. It is supposed that each neuron is coupled to all other neurons by electrical junctions and the synaptic delays are explicitly included. It is also assumed that all neurons are equal and interact via synapses of equal efficiency. This is justified if the neurons are assumed to occupy nearby positions in the brain cortex. For example, such a collection of similar neurons would be found in a patch of the brain cortex monitored by a single electrode of an EEG measurement. Another possibility, which could also be analyzed by the methods of this paper, would be to assume random uniform distributions with small fluctuations of the internal parameters, the interaction constants, and the time-lags.

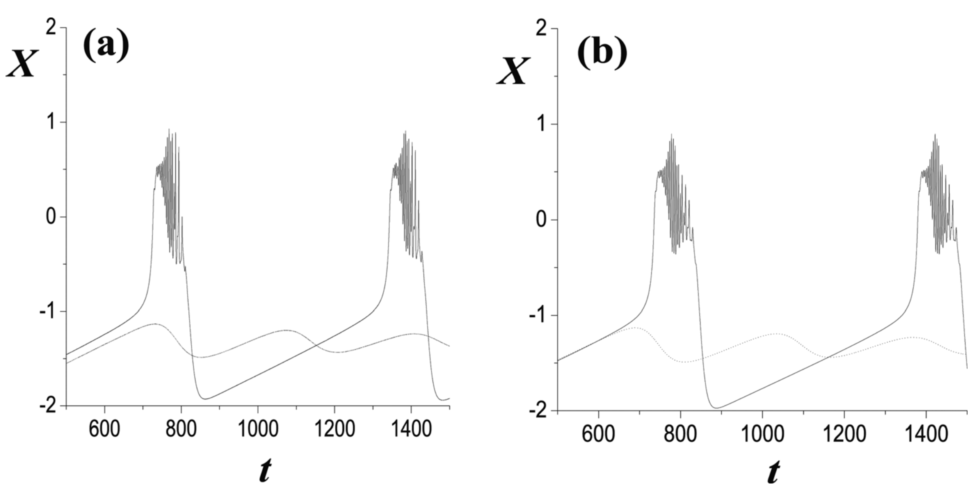

FIG. 8. Illustrates that, for $N = 70$, the bifurcation value of the parameter I, which implies destabilization of the stationary state and the transition to the bursting dynamics of the global variables in the exact system (a), is predicted by the approximated model (b) with the accuracy better than two percent. Accuracy for smaller N is commented in the main text. The parameters are $I = 1.275$ (dotted), $I = 1.295$ (full), and $c = 1$, $D = 0.001$, $\tau = 8$.

Thus, the model is given by a large set of stochastic delay-differential equations. We have focused on the dynamics of the collective variables represented as the spatial averages of the local ones.

Typical assumptions of the mean field approach are used to derive the set of nine deterministic delay-differential equations for the first and the second moments of the collective variables. The main assumption in the derivation is that the system represents an ensemble of Gaussian distributed independent random variables. One expects this to be a plausible assumption if the intensity of the noise and the coupling are not very large.

Various bifurcations due to variations of different parameters I, c, τ, D are observed in the dynamics of global variables of the exact system with large number of units, and the bifurcation values are compared with those predicted by the approximate model with only nine deterministic equations. It is observed that variations of any of the parameters I, c, τ, D can destabilize the quiescent global behavior and introduce bursting. Domains in the parameter space corresponding to stable quiescent behavior or to the bursting of the collective variables of the large exact system are correctly predicted by the approximate model. The predictions of the approximate model become more accurate as the number of units is increased. In this sense, the approximate model represents a very useful tool for an efficient numerical treatment of the global dynamics of the large system of delayed coupled noisy bursters.

It would be interesting to extend this type of analysis on the system of bursters coupled by some model of the chemical synapse.

ACKNOWLEDGMENTS

This work was supported in part by the Ministry of Education and Science of the Republic of Serbia, under project Nos. 171017 and 171015. N.B. should also like to acknowledge the support and hospitality of the Abdus Salam ICTP.

[1]E. M. Izhikevich, *Dynamical Systems in Neuroscience*: *The Geometry of Excitability and Bursting* (MIT, Cambridge, MA, 2005).
[2]E. R. Kandel, J. H. Schwartz, and T. M. Jessel, *Principles of Neural Science*, 3rd ed. (Elsevier, New York, 1991).
[3]H. Haken, *Brain Dynamics: Synchronization and Activity Patterns in Pulse-Coupled Neural Nets with Delays and Noise*, (Springer-Verlag, Berlin, 2006).
[4]H. D. I. Abarbanel, R. Huerta, M. I. Rabinovich, N. F. Rulkov, P. F. Rowat, and A. I. Selverston, Neural Comput. **8**, 1567 (1996).
[5]M. Dhamala, V. K. Jirsa, and M. Ding, Phys. Rev. Lett. **92**, 074104 (2004).
[6]N. Burić and D. Todorović, Phys. Rev. E **67**, 066222 (2003).
[7]E. Rossoni, Y. Chen, M. Ding, and J. Feng, Phys. Rev. E **71**, 061904 (2005).
[8]D. V. Ramana Reddy, A. Sen, and G. L. Johnson, Phys. Rev. Lett. **80**, 5109 (1998).
[9]S. H. Strogatz, Nature (London) **394**, 316 (1998).
[10]O. V. Popovych, C. Hauptmann, and P. A. Tass, Phys. Rev. Lett. **94**, 164102 (2005).
[11]C. E. Smith, in *Single Neuron Computation*, edited by C. Koch and I. Segev (MIT, Cambridge, MA, 1989).
[12]A. Longtin, Phys. Rev. E **55**, 867 (1997).
[13]B. Lindner, J. Garcia-Ojalvo, A. Neiman, and L. Schimansky-Geier, Phys. Rep. **392**, 321 (2004).
[14]E. V. Pankratova, A. V. Polovinkin, and B. Spagnolo, Phys. Lett. A **344**, 43 (2005).
[15]D. Valenti, G. Augello, and B. Spagnolo, Eur. Phys. J. B **65**, 443 (2008).
[16]A. S. Pikovsky and J. Kurths, Phys. Rev. Lett. **78**, 775 (1997).
[17]C. W. Gardiner, *Handbook of Stochastic Methods for Physics, Chemistry and the Natural Sciences* (Springer-Verlag, Berlin, 1985).
[18]L. E. Elgolc and S. B. Norkin, *Introduction to the Theory of Differential Equations with Deviating Arguments* (Nauka, Moscow, 1971), Chap. 5 (in Russian).
[19]X. Mao, *Exponential Stability of Stochastic Differential Equations* (Marcel Dekker, New York, 1994).
[20]X. Liao and X. Mao, Stoch. Anal. Appl. **14**, 165 (1996).
[21]S. Blythe, X. Mao, and A. Shah, Stoch. Anal. Appl. **19**, 85 (2001).
[22]J. Sun and L. Wan, Phys. Lett. A **343**, 331 (2005).
[23]D. S. Goldobin, M. Rosenblum, and A. Pikovsky, Physica A **327**, 134 (2003).
[24]D. S. Goldobin and A. Pikovsky, Physica A **351**, 126 (2005).
[25]N. Burić, K. Todorović, and N. Vasović, Phys. Rev. E **75**, 026209 (2007).
[26]N. Burić, K. Todorović, and N. Vasović, Chaos, Solitons Fractals **40**, 1127 (2009).
[27]Y. Shinohara, T. Kanamaru, H. Suzuki, T. Horita, and K. Aihara, Phys. Rev. E **65**, 051906 (2002).
[28]M. Sainz-Trapaga, C. Masoller, H. A. Braun, and M. T. Huber, Phys. Rev. E **70**, 031904 (2004).
[29]G. C. Sethia, J. Kurths, and A. Sen, Phys. Lett. A **364**, 227 (2007).
[30]G. Chun-Biao, M. Perc, and W. Qing-Yun, Chin. Phys. B **19**, 040508 (2010).
[31]Q. Wang, M. Perc, Z. Duan, and G. Chen, Phys. Rev. E **80**, 026206 (2009).
[32]Q. Wang, M. Perc, Z. Duan, and G. Chen, Chaos **19**, 023112 (2009).
[33]Q. Wang, Z. Duan, M. Perc, and G. Chen, Europhys. Lett. **83**, 50008 (2008).
[34]Q. Wang, M. Perc, Z. Duan, and G. Chen, Physica A **389**, 3299 (2010).
[35]Q. Wang, G. Chen, and M. Perc, PLoS ONE **6**, e15851 (2011).
[36]R. Rodriguez and H. C. Tuckwell, Phys. Rev. E **54**, 5585 (1996).
[37]S. Tanabe and K. Pakdaman, Phys. Rev. E **63**, 031911 (2001).
[38]M. A. Zaks, X. Sailer, L. Schimansky-Geier, and A. B. Neiman, Chaos **15**, 026117 (2005).
[39]H. Hasegawa, Phys. Rev. E **68**, 041909 (2003).
[40]H. Hasegawa, Phys. Rev. E **70**, 021911 (2004).
[41]H. Hasegawa, Phys. Rev. E **70**, 021912 (2004).
[42]A. Pototsky and N. Janson, Int. J. Bifurcation Chaos **20**, 1825 (2010).
[43]N. Burić, K. Todorović, and N. Vasović, Physica A **389**, 3956 (2010).
[44]N. Burić, K. Todorović, and N. Vasović, Phys. Rev. E **82**, 037201 (2010).
[45]J. L. Hindmarsh and R. M. Rose, Proc. R. Soc. London, Ser. B **221**, 87 (1984).
[46]X.-J. Wang, Physica D **62**, 263 (1993).
[47]M. Perz and M. Marhl, Phys. Rev. E **71**, 026229, (2005).
[48]N. Burić and D. Ranković, Phys. Lett. A **363**, 282 (2007).
[49]I. Belykh, E. de Lange, and M. Hasler, Phys. Rev. Lett. **94**, 188101 (2005).
[50]R. E. Lee DeVille, E. Vanden-Eijnden, and C. B. Muratov, Phys. Rev. E **72**, 031105 (2005) .
[51]For the package documentation, containing a detailed description of the set of routines with the appropriate examples, see what is available at http://www.math.pitt.edu/~bard/xpp/xpp.html.
[52]K. Engelborghs, T. Luzyanina, and G. Samaey, Technical Report TW-330, Department of Computer Science (K. U. Leuven, Leuven, Belgium, 2001).
[53]K. Engelborghs, T. Luzyanina, and D. Roose, ACM Trans. Math. Softw. **28**, 1 (2002).

Chaos is copyrighted by the American Institute of Physics (AIP). Redistribution of journal material is subject to the AIP online journal license and/or AIP copyright. For more information, see http://ojps.aip.org/chaos/chocr.jsp